19th International Conference on
Adaptive Structures and Technologies
October 6-9, 2008
Ascona, Switzerland

Biomimetics in airship design

S. Michel[1]*, Ch. Jordi[1], L. Wahl[2], N. Widmer[2], Erich Fink[3], L. Kniese[4] and A. Bormann[5]
[1] Swiss Federal Laboratories for Materials Testing and Research (Empa), Duebendorf, Switzerland,
[2] Swiss Federal Institute of technology, Zuerich, Switzerland,
[3] Technical University Berlin, Berlin, Germany,
[4] Evologics GmbH, Berlin, Germany,
[5] AeroiX GmbH, Kleinmachnow, Germany.
* Corresponding author: S. Michel, Ueberlandstrasse 129, CH-8600 Duebendorf, Switzerland
Tel: +41 - (0)44 823 45 88, Fax: +41 - (0)44 823 40 11, E-mail: silvain.michel@empa.ch

ABSTRACT

Many attempts have been made to mimic the movement of a fish in water in order to find novel solutions in autonomous underwater vehicles (AUV) [1-4]. Conventional airships are driven by propellers and steered by stabilizers with rudders or with thrust vector control. Such propulsion and steering systems are efficient only in a small range of operation. The goal of our project is to mimic the fish-like movement with an airship body in air. In a theoretical study [5] we have shown that a 6m long airship in air is similar to the trout in water. Therefore we want to build a geometrically similar body which mimics the body motion of a trout in steady state swimming. The activation is realized using Dielectric Elastomers (DE), a promising class of Electroactive Polymers (EAP). The principles of biomimetics in structural design and propulsion are discussed in this paper. The similarity of the optimized solutions found by the evolution for animals living in water and an optimized design of an airship will be shown. In a next step, the design of an indoor-flying airship propelled by a fish-like motion is evaluated. Various development tests, including wind tunnel testing and flight trials were performed and the gained results will be presented. First computational fluiddynamic simulations performed have shown similar vortex flow fields. In addition, the average forces could be measured accurately in wind tunnel tests and will be used to dimensioning the activation of the fin appropriately. From these results a conclusion shall be drawn, how far biomimetics can be used successfully in the design of future airship.

Keywords: Biomimetics, airship, active structures, electroactive polymers, dielectric elastomers

1. INTRODUCTION

Lighter-Than-Air vehicles are a promising class of transport systems for heavy cargo, stratospheric platforms, but also for surveillance or animal observations. In the last decades various concept studies have been performed for stratospheric platforms, which are interesting alternatives for land-based networks as well as for satellites in telecommunication, reconnaissance and observation [6-10]. Classical propulsion systems composed of piston engines with gears and propellers show a limited efficiency due to thermo mechanical losses in the engine, mechanical losses in the gears and fluid dynamical restrictions of the propellers. In addition these systems are noisy and if driven by piston engine have a negative impact on the environment by pollution. These

disadvantages can be grave, for they prohibit some new applications such as stratospheric platforms (energy efficiency) [10], animal observations or surveillance (noise). New systems should be energy efficient, noiseless and environmentally friendly. Our idea in this context is to apply biomimetic principles.

2. THEORETICAL FEASABILITY

The method of mimicking biological forms and concepts in the development of technical products has a long tradition. A pioneer in biomimetic aerospace design was Hertel, who already in 1963 was studying natural forms of various fishes for efficient fuselage designs and alternative propulsion systems for airplanes [11]. Later Bannasch for example analyzed in detail living penguins and their bodies, which have an extraordinary low drag coefficient [12, 13]. His results were first used for an airship design by the Technical University of Berlin in 1998 in the airship called "Luftfisch". The shape of this 10m long semi-rigid airship is basically a rotational symmetric shape of a penguin. We went one step further, when we suggested not only to adapt the form of a fish (in order to reduce the drag), but also its motion as an efficient propulsion system [5, 14]. The main motivation for such a new concept for the propulsion of an airship is its much better efficiency.

2-1. Propulsion Efficiency Considerations

Considering a conventional propeller driven rigid airship (Fig. 1), the thrust is generated quite inefficiently by propellers that are mounted sidewise of the body. The size of the propellers' diameters is fairly limited to avoid supersonic relative tip mach numbers. Consequently, the air has to be accelerated quite significantly in order to generate enough momentum to compensate the drag due to body friction and the wake behind the airship in case of boundary layer separation. The momentum which is produced by a propeller and the momentum loss induced by the flow resistance of the airship body can be calculated with following equations [11]:

$$F_T = \int (\rho u_T (u_T - u_0) \delta A \tag{1.a}$$

$$F_R = \int (\rho u_R (u_R - u_0) \delta A \tag{1.b}$$

The reason for the low efficiency of these kind of thrust generation is the high velocity of the propeller air jet u_T.

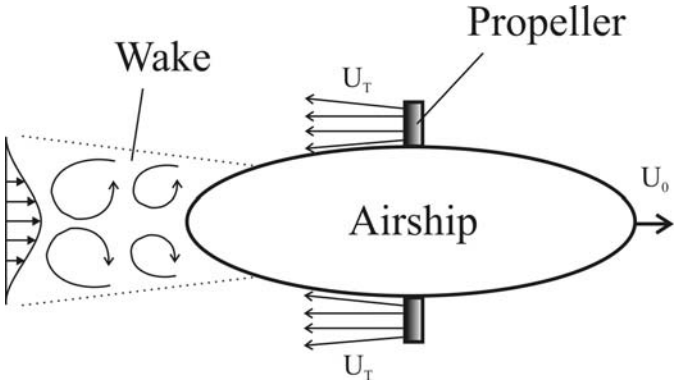

Figure 1. Schematically sketched rigid airship with conventional propulsion by propellers.

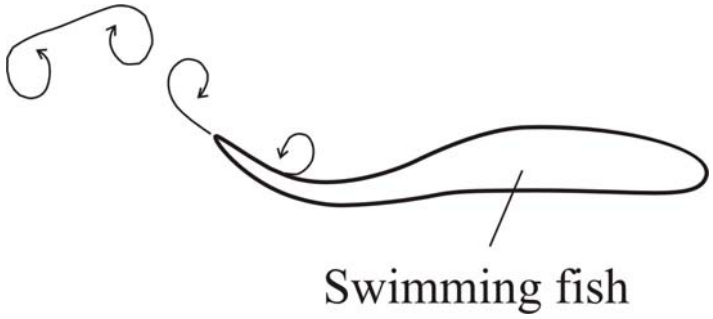

Figure 2. Schematically sketched fish with propulsion by undulating body motion and fin stroke.

In case of a swimming fish (Fig. 2) the thrust is generated by body undulation and/or by caudal fin flapping. The major advantage of this propulsion concept is that thrust is generated at the same location where body induced momentum loss occurs. The rigid fish body causes a wake flow which is in direct correlation to momentum loss (Eq. 1.b). In order to obtain a trust at constant speed, this momentum loss has to be compensated by the propulsion mechanism. Consequently, in this case there is no relative velocity between the flow behind the fish body and the surrounding fluid, which manifests in a vortex line that is fixed in space. Hertel [11] conducted a thought experiment to illustrate the efficiency advantage of fish-like propulsion. There are two different configurations to compensate a momentum loss of a flow caused by resistance. The first possibility is to use a thrust generator (propeller) in parallel with the decelerated fluid. The other way is to set it in series. He verifies his statement that the required power is reduced if the locations of momentum loss and thrust generation fall into one another with following calculations:

$$P_p = F_R(u_0 + u_T)/2 \text{ (in parallel configuration)} \quad (2.a)$$

$$P_S = F_R(u_0 + u_R)/2 \text{ (in series configuration)} \quad (2.b)$$

In the first configuration, the propeller has to accelerate the fluid from u_0 up to u_T in order to compensate the momentum loss. In the second configuration, after deceleration of the fluid to u_R, it is accelerated up to u_0 again. It is obvious, that u_R is smaller than u_T. Therefore P_S is smaller than P_P as well. Hertel [11] predicted a power reduction of up to 60%. In Fig. 3, which is adapted from Fish and Lauder [15] the propulsive efficiencies of a marine propeller and different whales are compared.

It shows that the efficiency of fish-like locomotion is significantly higher and also for a broad range of thrust coefficient almost constant. The propeller system has only at one specific thrust coefficient a maximum and decays drastically to both sides of the maximum. These interesting findings are not only valid in water, but when correctly transformed also in air.

If the shape and motion of swimming fish in water is to be transferred to an airship in air, fluiddynamic similarity theorem has to be considered.

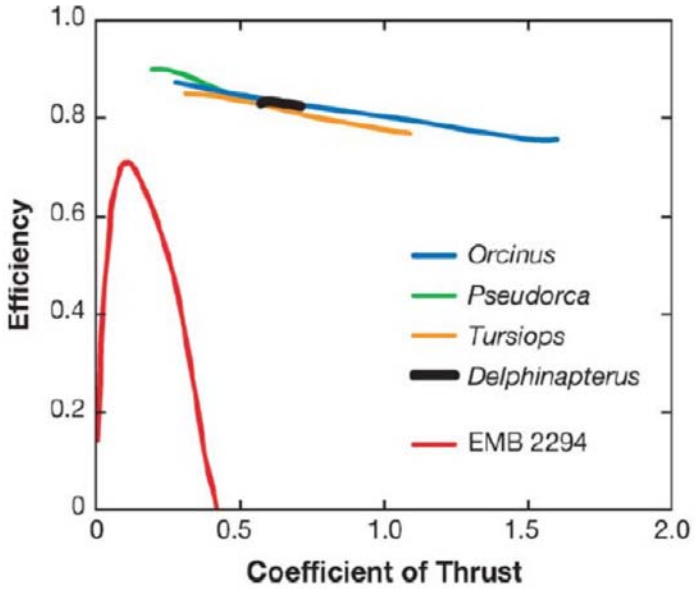

Figure 3. Comparison of relationships of propulsive efficiency and thrust coefficient for 4 species of small whales and a typical marine propeller [15].

2-2. Similarity and dimensional analysis

In the following analysis we assume a 6 meter long airship flying with a steady state velocity of 1 m/s in a standard atmosphere (23°C, 1023 hPa).

In order to be able to apply the locomotion mechanism of a fish in water to a deformable airship in air, the fluiddynamic conditions as well as the geometrical shape of fish and airship have to be similar. In general, two scenarios are fluid dynamically similar, if - strictly speaking - all the following non-dimensional parameters are equal:

(a) Reynolds number
(b) Mach number
(c) Strouhal number
(d) Froude number

However, in a specific case it is not important, that all of these parameters are exactly equal. Therefore a ranking of the importance of these parameters has to be made. The Froude number correlates the inertial with gravitational forces, e.g. this number must be considered in cases, where gravitational forces are significant. We can ignore this number, because we are considering here primarily horizontal swimming and flying. What Mach number is concerned, we have to consider the flight speed compared to the speed of sound. Because the flight speed of the airship is very small compared to the speed of sound, it means firstly, that the Mach number will be close to zero and secondly, that the surrounding air flow can be assumed to be incompressible. The ratio of inertial to viscous forces is known as the Reynolds number. If the Reynolds number is low (less than 10^3) viscous forces are large compared to inertial forces and therefore inertial forces can be neglected. If the Reynolds number is large (larger than 10^6) viscous forces are small compared to inertial forces and therefore viscous forces can be neglected. It will be calculated here with respect to the whole body length:

$$\mathrm{Re} = \mathrm{u}_0 L \frac{\rho}{\mu} = 1 \cdot 6 \cdot \frac{1.0}{16.6 \cdot 10^{-6}} = 0.36 \cdot 10^6 \qquad (3)$$

Hence, none of the two conditions mentioned above are satisfied. Therefore it can be concluded that the viscous forces are of the same order of magnitude as the inertial forces. One condition of similarity is thus, that the Reynolds number must be equal.

The Strouhal number is the ratio of the forces due to unsteady flow and forces due to steady flow. Obviously this is the non-dimensional parameter which plays the major role for the fluid dynamical similarity in our case. The Strouhal number is defined as:

$$\mathrm{St} = \frac{Df}{u_0} \tag{4}$$

Where D is a typical dimension of the vortex street generated in the wake of the body, f is the stroke frequency and u_0 is the cruising speed of the object. Because D is not an a priory known value, usually the Strouhal number is calculated with the peak-to-peak stroke amplitude of a reference point (the trailing edge of the tail fin) instead of D. Other definitions have also been used, such as the depth of the tail fin [16], or even the full length of the fish [11]. Following Triantafyllou [17] we will us the Strouhal number based on the peak-to-peak amplitude, 2a:

$$\mathrm{St}' = \frac{2af}{u_0} \tag{5}$$

The importance of the Strouhal number in efficient swimming of fish has been reported in numerous studies, see for example [18-21].

2-3. The trout as a model for a 6 meter long airship

From the various fishes we want to find one, which would be a meaningful model for our airship. In a first step we will focus on fluiddynamic aspects and ignore restrictions due to aerostatic or due to the structural set-up. Considering the fluiddynamic similarity, the first requirement is a Reynolds number of $0.36 \cdot 10^6$. Nägele has collected fluiddynamic data of various species in water [21] and we found for example the tuna and the rainbow trout, which are swimming with such a Reynolds number. This can be seen by the following calculation for the trout: The trout is 0.3 m long, and reaches a steady state swimming speed in water of 1.2 m/s. With L = 0.3 m, v_∞ is 1.2 m/s, and ρ is $1.0 \cdot 10^3$ kg/m3 and μ is $1.002 \cdot 10^{-3}$ kg/ms for water, the Reynolds number is:

$$\mathrm{Re} = u_0 L \frac{\rho}{\mu} = 1.2 \cdot 0.3 \frac{1.0 \cdot 10^3}{1.002 \cdot 10^{-3}} = 0.36 \cdot 10^6 \tag{6}$$

Both are very efficient swimmers. Looking at the fish geometry as a design model for a deformable airship, the rainbow trout seems to be a promising shape for the airship because of its laminar formed body. Additionally, the efficient propulsion is combined with a good manoeuvrability, which also important for airships. On the other hand the tuna has an even more efficient lift-based propulsion mechanism compared to the trout, with a minimized tendency to side slipping and yawing of anterior body due to inertial recoil. However this fish is known to have a low efficiency at low speeds and bad manoeuvrability. Therefore we decided to use the rainbow trout as a design model for

further studies on our airship design.

The shape of a rainbow trout has a width-to-body length ratio of approx 14% and a height-to-body length ratio of approx. 22%, see Fig. 4. [11]. The maximum width and height is at 40% of the body length. Analytically, this shape can be approximated by a NACA0014-Profil in the x-y plane and NACA0022 in the x-z-plane. Such shapes are known to have very low drag coefficients. The body cross section can be assumed to be elliptical. In this way, we can take the trout as a model for the undeformed shape of the airship.

If we follow the paradigm of biomimetic, e.g. that nature has found not only optimized forms but also the corresponding optimized motion pattern [22], we can choose the motion pattern of the trout also for our airship in air. The wake of a rainbow trout has been studied using stereoscopic digital particle image velocimetry [23]. The motion pattern of a trout has been measured for example by Webb [24]. The lateral amplitude increases along the fish from head to tail. Interestingly the amplitude is not zero at the forward and middle part of the body. The propulsive elements near the tail have a much larger thrust component due to greater traverse distance and larger speed which results in more water acceleration. Additionally, the propulsive elements are oriented more toward the fish swimming direction in the aft part [25].

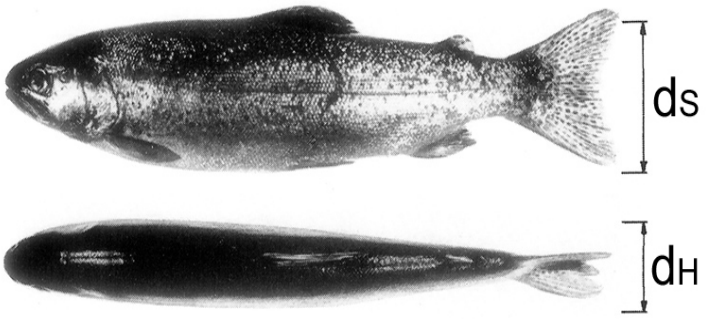

Figure 4. Typical undeformed shape of a trout [11].

If we analyze the body motion of the steady state swimming we find the following typical values: The amplitude of the fin stroke is 20% of the length. The stroke frequency f is 4.5 Hz and the resulting swimming speed u_0 is 1.2 m/s. With these values we find a Strouhal number of 0.45. A polynomial function representing the increasing lateral amplitude from the head to the tail can be defined, see for example Webb [24]. For simplicity in our case we used a quadratic function as a first order approximation. Therewith the caudal fin stroke frequency is exemplarily calculated: With St' = 0.45, a = 20% of 6 m = 1.2 m and u_0 = 1 m/s. The stroke frequency is:

$$f = \frac{St' \cdot u_0}{2a} = \frac{0.45 \cdot 1}{2 \cdot 1.2} = 0.1875 \cong 0.2Hz \tag{7}$$

The adaptation of the fish-like locomotion mechanism in water to a deformable airship in air should be possible, if these geometrical and fluid dynamical similarities are satisfied. The Reynolds number with respect to body length and the Strouhal number are the non-dimensional parameters of relevance to meet fluid dynamical similarity. Therefore we can conclude that a full grown rainbow trout is a meaningful design model for the deformable airship.

2-4. The Structural Concept of the biomimetic airship

The structural concept of a deformable airship is a highly multidisciplinary challenge. In contrast to the trout in water, an airship has to compensate its weight with the aerostatic lift produced by a lighter-than-air gas. The requirement of buoyancy does not allow slender shapes, because they have a small volume-to-surface ratio, which reduces the payload capacity. This is in direct contrast to the requirement of maximum speed and efficiency, which is better the more slender the body is. In addition in airship design the shape of the body can not be chosen free from structural restrictions. In case of a rigid airship the structural weight is much larger than the hull weight. Therefore for smaller airship this approach is not feasible and a non-rigid design is favourable. In case of non-rigid airships, the shape is defined by the hull geometry and the internal pressure. If we consider further the undulatoric propulsion mechanism we have to increase lateral area in order to have enough contact area between the body and the fluid. One possibility is to have a height-to-width ratio of 3 – 4, seen in Fig. 4 or to add fins in the symmetry plane, shown in Fig 16. Finally all the requirements mentioned above have to be fulfilled in one design.

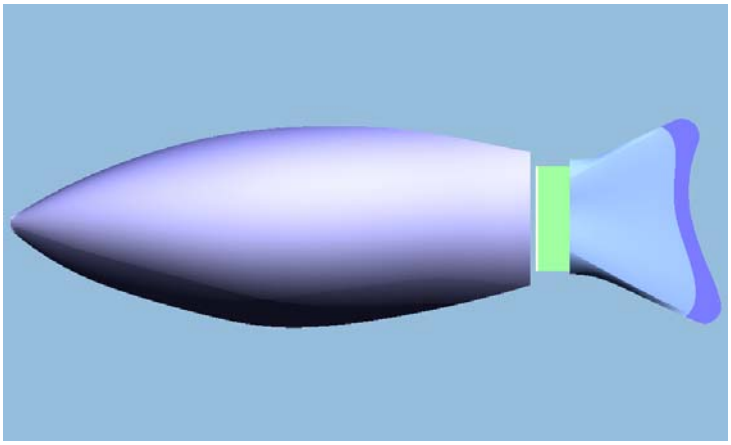

Figure 5. Design concept of the biomimetic airship.

Our design concept is a balanced compromise between these requirements. The basic dimensions are a total length of 6.6m, the maximum height is 1.9m and the width is 1.5m, see Fig. 5. It consists of a pressurized body with an internal rigid multi-body structure in the symmetry plane. This structure elongates the cross sections in the vertical direction, which results in a larger height than width. The body is flexible in the symmetry plane at least at one cross-section. At this position an active body segment allows to bend the pressurized body of the body actively. A first estimation of the weights and the balance of this design proposal is given in Table 1.

The tail-fin is a compliant non-pressurized flat plate with Fin Ray Effect®. The Fin Ray Effect® has been found in tail fins of fishes by Leif Kniese [26]. The kinematic of such a structure allows a strong interaction of the structure with the fluid. The importance of flexibility of fins for propulsion has been reported for example in [27]. In case of a structure with Fin Ray Effect®, the combination of the lateral pressure distribution and the forces introduced as a pair at the root of the fin results in large S-shaped deflections of the whole fin, see Fig. 6. The activation of the tail fin has in principle three degrees of freedom: the first one is a flapping motion (translative motion) of the root, the second one is a rotation of the root and the third one is the activation of the Fin Ray Effect®, which results, in a variation of the S-shape of the fin. In our case due to simplification we will only activate two of them: The translative motion and either the rotational motion or Fin Ray Effect ® (The decision will be made based on wind tunnel tests). The translative motion will be realized by the bending motion of the active body segment (described in detail in section 3.1). The second motion will be realized by the actuator module located between the body and the fin (green box in Fig. 5, see

also section 3.2).

Table 1. Estimation of weights and balance for the proposed biomimetic airship design.

Component	Structural weight	Position from tip
Passive envelope	513 g	250 mm
Active material in the envelope	260 g	375 mm
Internal structure	1750g	250 mm
Gondola, with engines, electronics	2150g	60 mm
Activation module for the tail fin	650g	511 mm
Tail fin	590g	640 mm
Payload and trim weight	200 g	60 mm
Total weight (= aerostatic lift)	6120 g	250mm

The actuation technology necessary in order to get the body deformation described above will be obtained through the application of Dielectric Elastomer (DE) membrane actuators. Dielectric Elastomers are one material class of Electroactive Polymers (EAPs) and are promising material systems as actuators in active structures, where large deformations are required. They transform electrical energy directly to mechanical work and produce large strains (20% and more). Especially Dielectric Elastomers were shown to have good overall performances. Pressures of 16.2 MPa, free area strains of 215% and specific elastic energy densities of 3.4 J/g could be shown [28].

A DE actuator is basically a compliant capacitor, where a passive elastomer film is sandwiched between two compliant electrodes. When an electrical voltage is applied, the electrostatic forces arising from the charge displacement on the electrodes squeeze the elastomer film. This electrode pressure mechanically loads the polymer film. Because such elastomers are essentially incompressible the area of the capacitor is enlarged. As soon as the voltage is switched off and the electrodes are short-circuited the capacitor contracts back to its original shape.

With this technology membrane- or shell-like structures can be created witch integrated actuator and load-carrying functionality. The electro mechanical behaviour of a functional model of an “active envelope” was studied, [29]. An active envelope is the combination of such a DE membrane actuator mounted on an airship envelope. Mechanically it is a multilayer membrane, with a lightweight and helium-tight membrane, which is characterized by a high tensile strength and a high compressive compliance, and a DE-actuator consisting of at least one prestretched dielectric film layer coated on both sides with compliant electrodes. The basic idea of this structural element is illustrated schematically in a force-versus-deformation diagram, see Fig. 8.a. During the manufacturing process the over-stretched DE-actuator is attached directly to the tight airship envelope (point 1). If the actuator exerts a resulting tension force larger than that induced by the internal pressure in the envelope, the membrane below the DE-actuator will wrinkle (from point 1 to 2 on the line denoted as “passive DE”). By applying an electrical voltage to the DE-actuator, the DE actuator is enlarged and the envelope segment regains its fully elongated state (point 3 on the line denoted as “active DE”). The slope of both lines represents the stiffness of the DE actuator. If the internal pressure is too high, then the envelope is always tight and the stiffness of the system is the stiffness of the envelope (steep lines beyond point 1).Therefore it is important to justify the internal pressure such that the full deformation range (difference between point 2 and 3) is possible.

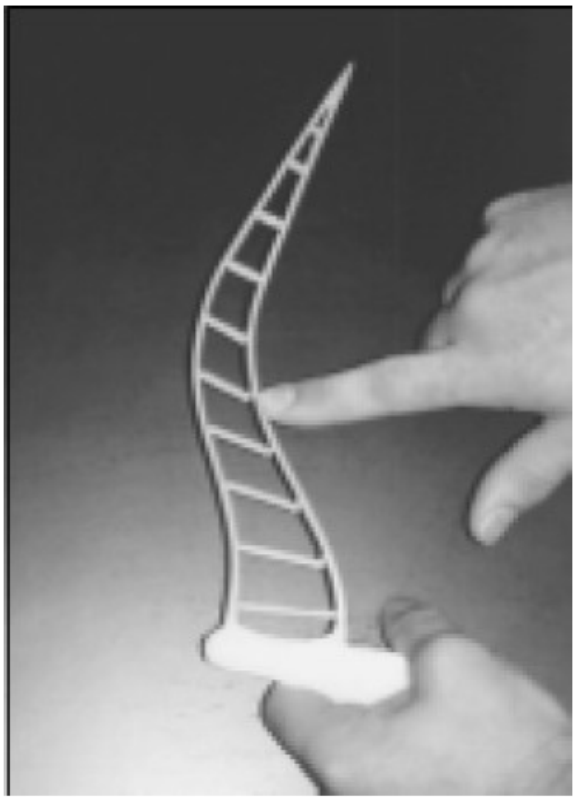

Figure 6. Demonstration of the Fin Ray Effect®.

In a theoretical study the membrane stresses and strains of such an "active envelope" for an airship body slightly pressurized and deforming like a trout have been analyzed. In order to experimentally simulate the stress state of the airship envelope, a functional model of the active envelope was defined and experimentally characterized. With this cruciform planar functional model mounted on an in-house made testing device the deformations on activation under representative membrane stresses could be measured, see Fig. 8.b. Therewith the feasibility of the proposed concept could be investigated. The line loads on each arm of the cross were determined to represent the stress distribution in the slightly pressurized (300 Pa) airship. These line loads were calculated for a 6m x 3m x 1m elliptically shaped body. The line loads vary with orientation and location from 160 N/m in the longitudinal direction at the thickest section to zero at the nose and the tail. The circumferential line load varies from 80 N/m to zero respectively. The ratio between longitudinal and circumferential line loads is between 1 and 2. Furthermore, the envelope strain and strain rate requirements for steady (and accelerated) swimming were also defined. The required local deformations of the envelope were derived from the analysis of the deformed fish body. The maximum strain of the steady state swimming mode was 15.1% in longitudinal direction.

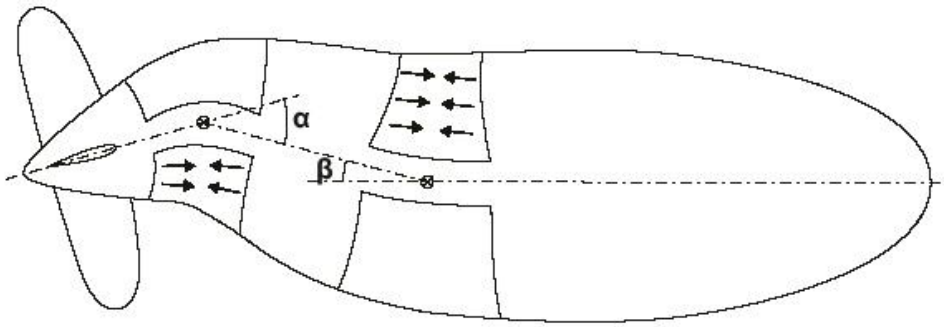

Figure 7. : Schematic of deformed shape of an airship, mimicking the motion of the fish body

The envelope material Nonex® (detailed description, see below) satisfied the basic mechanical and aerostatic requirements. Thanks to its small thickness (25 μm), it can be wrinkled easily. The metal coating grantees the required Helium tightness. The envelope can be cut in segments that are successively welded together in order to achieve a Helium-tight body with high compliance under compression forces.
The largest longitudinal activation strain was achieved by the active envelope with a (6.5, 3)-over-stretched DE-actuator. It reached 13.5% at an activation voltage of 3.5kV. This was reached under a biaxial line load ratio of 2.37. The strain could even be increased through a higher electrical activation voltage. An extrapolation of the measured data results in an activation strain of 16% at approx. 3.8kV, which satisfies the lateral strain requirement of 15.1% for steady swimming. Furthermore, the reduction of the transversal load not only allows to increase the longitudinal activation strain, but also to decrease the line load ratio from 2.37 to 2. Thus, the requirement for the airship line load ratio could be fulfilled. The membrane line load requirement of 160 N/m at $\Delta p = 300$ Pa and 80N/m can be fulfilled through the stacking of eight DE-actuators. These experimental results allow concluding that the proposed concept for an active envelope is feasible at least for the steady swimming mode.

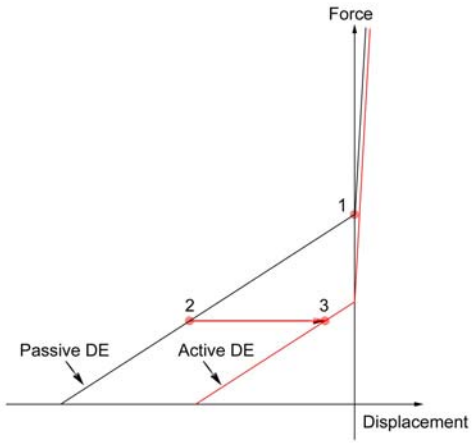

Figure 8.a. Force versus displacement behaviour of an active segment of the envelope.

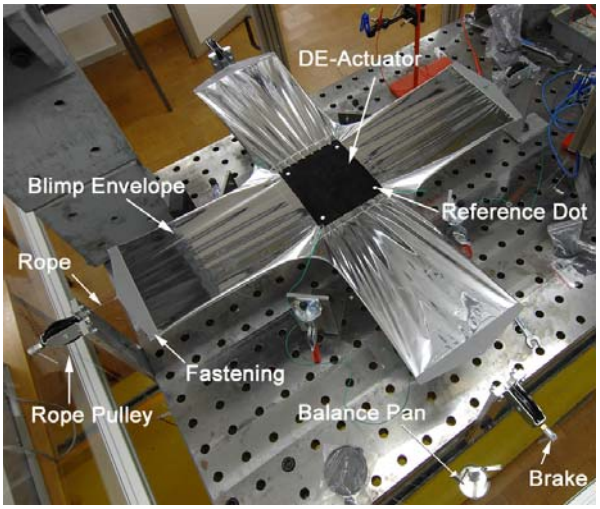

Figure 8.b. Biaxial tension test set-up for the active segment of the envelope.

2-5. Computational Flow Simulations

Based on the methodology developed in reverse engineering of self-propelled anguilliform swimmers [22], the fish-like motion has been simulated with a simplified geometrical representation of the design proposal. The lens or plate formed cross-sections of the original body have been transferred into elliptical shapes. The motion has been parameterized as a wave of curvature κ travelling along the centreline of the body:

$$\kappa(\mathrm{s},\mathrm{t}) = \mathrm{K}(s)\sin\left[2\pi(t/T - \tau(s)\right] \tag{8}$$

Where K(s) is the curvature amplitude, which is modulated by a sine-wave with period T and phase shift τ(s). With these parameterization continuous deformations of the body, discrete hinges, as well as active or passive tail fin deformations can be modelled effectively. As a reference case K(s) and τ(s) were chosen to represent the motion pattern of a trout in steady state swimming, as described

in section 2.3.

The system of the deforming body interacting with the surrounding fluid is described by the 3D incompressible Navier-Stokes (NS) equations that are coupled to Newton's equations of motion for the self-propelled body. The NS equations are solved using the Finite Volume package STAR-CD v. 3.15 extended with user subroutines for the fluid-body coupling [22].

The current approach allows calculations at a maximum Re_{UL} of approx. 3000. Note that this Re number is several orders of magnitude lower than the Re number of the airship. Nevertheless the computational model can provide valuable information for critical decisions for the design of the biomimetic airship. An extensive study of this flow is the subject of ongoing work [30] addressing questions such as: How does a design with discrete hinges compare to a continuously deforming body? What is the effect of the deflection angle and phase shift of a flexible tail fin on the swimming performance?

For the case with one discrete hinge and a stiff tail fin the general structure of the wake remains similar to the results reported in Fig. 9. We find that simplifying the motion with a single hinge and a stiff tail fin still allows similar swimming speeds if the tail beat amplitude is slightly increased compared to the case with continuous deformation. Investigations with modelled fin flexibility show that the highest efficiency is achieved when the fin bending has a phase lag of roughly pi/2.

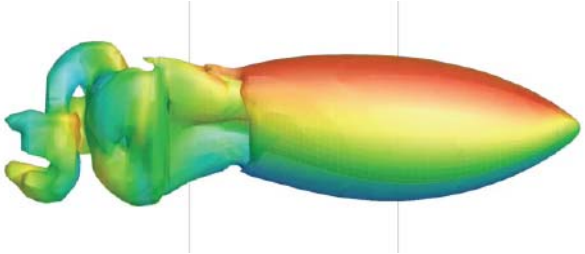

Figure 9. Vorticity iso-surfaces coloured with span wise vorticity of the trout motion pattern.

3. PRACTICAL FEASABILITY – RESULTS OF DEVELOPMENT TESTS

In the second part of the work the structural elements of the biomimetic airship with a fish-like propulsion system were developed. The following parts of the development are completed:

1) An active body segment
2) Active hinge for the actuation of the tail fin
3) Design of a tail fin with Fin Ray Effect®

In the following sections the results of these studies will be summarized.

3-1. The active body segment

The goal of this work package was to develop and characterize an active body-segment based on DE membrane actuators. Based on the feasibility study on the active envelope, [29], the next step was to build a pair of actuators positioned at each side of the pressurized body, see Fig. 10.a. For that purpose slightly curved prestretched VHB-4910 actuators were mounted on a framework and activated alternately, see Fig. 10.b. In this approach the actuators are separated from the airship envelope to avoid undesirable friction between the envelope and the actuator. To characterize the active body-segment a test stand has been built-up. Dynamic measurements of the angle and static measurements of the force are taken of a single-layer and a double-layer functional model at various

frequencies. The single-layer prototype reached 13°, which is 90% of the required 14.5° deflection angle. By optimizing the electrical supply and reduction of friction in the hinge of the framework we expect to reach the required deflection angels.

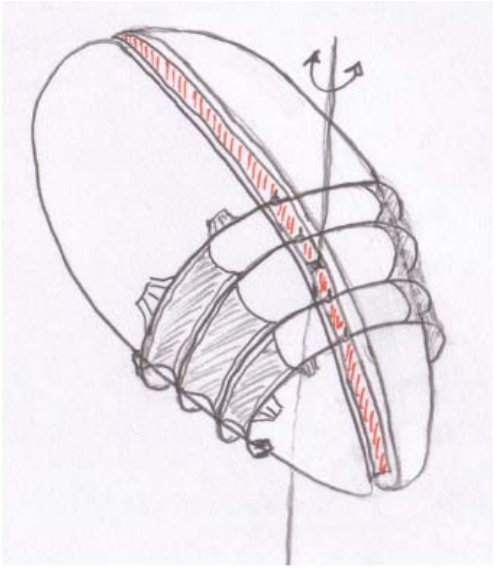

Figure 10.a. Schematic of the active body segment, with two pressurized half-bodies (white), the internal rigid structure (red), the pivot line (arrow) and the membrane actuators on each side (black dashed).

Figure 10. b.A single-layer membrane actuator in the test rig (black: active area)

3-2. The activation of the tail fin

In a second study the module for the activation of the tail fin (schematically represented by the green box in Fig. 5) was developed. In an earlier work a so called active hinge has been developed successfully for the activation of steering rudders, [31, 32]. Based on these results the next development step was to scale-up this design in order to increase the forces. A theoretical simulation tool has been used to define the dimensions and the shape of it. In order to define the required forces the aerodynamic loads on a flapping fin were estimated. The significantly non-stationary flow condition of a flapping fin was experimentally simulated by a rotation of a plate and measuring the moment needed for this movement and the calculation of the drag force of the same plate hold perpendicular to a stationary flow. On the other hand the force and moments of wind tunnel tests (see section 3.3) were also taken into consideration. The required activation moment at the hinge was found to be in the range of 1.75 to 3.0 [Nm]. Finally the dimensions of the active hinge were chosen to be 1m high, and 30cm deep with 4 layers of VHB-4910 DE membranes on each side, see Fig. 11. The active area on both sides was reinforced by thin carbon rods in order to hold the prestraining of the acrylic film in the vertical direction. In order to characterizing the electro-mechanical behaviour of this module, a test bed was built-up, where aerodynamic loads were simulated by two linear springs generating an external load linearly increasing with the deflection angle. Measured electrical signals (current and voltage) and the mechanical behaviour of the springs allowed defining the power consumption, the mechanical work done per activation half-cycle as well as the efficiency. A maximum hinge moment of 1.25 [Nm] at 20° deflection and 0.2 Hz was reached. This actuator allows generating 0.14W mechanical power. The results, which were realized, could meet in principle the requirements. The uncertainty in the assumption of the aerodynamic loads is not a critical point, because the forces generated can be scaled in the final design by the number of DE membrane layers on each side.

Figure 11. Full size functional model of the active hinge for the activation of the tail fin.

3-3. The aero-elastic tail fin

There is only a limited number of projects on oscillating foils or fins and to the knowledge of the authors they have been done all in water, see for example [33] and [34]. We have studied the design of an aero-elastic tail fin as an element of the undulatoric propulsion. Again with the theory of similarity it can be shown, that an elastic tail fin of such a 6 meter long airship is similar to a tail of a trout in water, if the dimensions of the fin and the deformation is geometrically similar. In Fig. 12 three tail fins are shown witch are technical simplifications of the natural model of a trout.

Fin A represents the tail fin of a trout (depth =0.175L, height = 0.35L, where L is the total length of the trout). Fin B represents the aft part of the body plus the tail (depth =0.36L, height = 0.41L). Both fins were fabricated as partly stiffened Depron-plate (thickness 5 mm and 9mm respectively). Fin C was a Fin with Fin Ray Effect® shaped like the natural tail fin. It was made from a carbon tube framework with a textile skin (depth =0.175L, height = 0.29L).

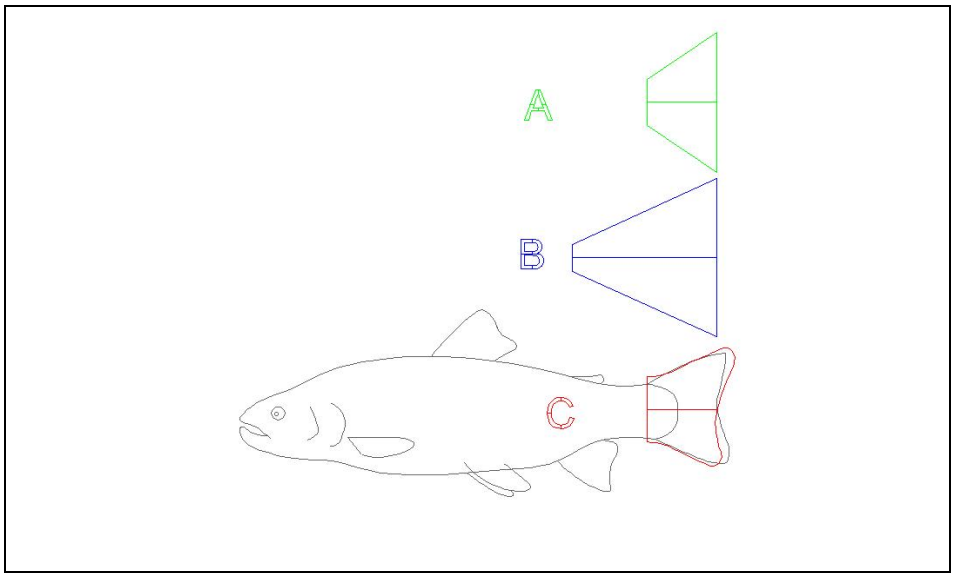

Figure 12. Shape and size of three tail fin design, tested in the wind tunnel.

A first series of wind tunnel tests have been performed, where these tree fins have been oscillating around a rod mounted on a 6 degree of freedom load cell (the scaling parameters are given in Table 2). The rod could be moved translative and in rotation independently. With this unique apparatus a fish-like motion could be generated. In these tests the translative and rotational amplitude, the frequency and phase shift as well as wind speed were varied systematically. The movement of the fin and the flow in the wake of it were monitored with a high-speed video camera. Based on the force and moment measurements with the load cell, the dimensionless propulsion or drag forces and the propulsion efficiency could be evaluated.

By analysing the high speed camera video streams, (see Fig. 13) both Strouhal numbers (defined in eq. 4 and 5) could be determined. The tests show, that only above a critical frequency of approx. 1 Hz propulsion is produced by the oscillating fin. The critical frequency is dependent on the type of fin (see Fig. 14), the ratio between translative and rotational movement and the phase shift between them (see Fig. 15.). The maximum of propulsion has been found with Fin C at maximum frequency of 2 Hz. However the best efficiency was found to be 23% at a frequency of 1.13 Hz with Fin B. The phase shift between translative and rotational movement has also a large influence on the propulsion. An optimum is found close to 72° also reported by Hertel [11].

In this first test series the Fin Ray Effect® in Fin C was not yet activated. In a second test series the Fin Ray Effect on propulsion force and efficiency will be explored in detail.

3-4. Functional models

With a model airship (Fig. 16) the undulatoric propulsion in air has been explored. The airship envelope was made of Nonex®, which is a polymeric multilayer structure especially developed for Lighter-than-Air vehicles.

This functional model was developed in order to verifying the practical feasibility of the undulatoric propulsion concept in air. While the wind tunnel tests gave first results on possible designs of fins and their performances the practical feasibility was still an open task. There are only a very limited number of airships that are propelled by a fish-like propulsion system: One is the “Air_ray” from FESTO, [35]. This free-flying object was a semi-rigid hybrid airship, with a lifting body filled with Helium in the centre section and flapping wings on each side. This airship was looking like and mimicking successfully the motion of a stingray. It was first shown at the

"Hannovermesse" in Hannover in 2007. Another one is a model blimp called "Wanda" shown by Martin Müller at the Wall-Halla indoor flying meeting 2008, [36]. However, none of these objects have been investigated scientifically.

Table 2. Scaling of the fin for the wind tunnel (typical numbers of the trout in water and design point of the model in the wind tunnel).

Parameter	Unit	Trout	Model
Fluid		water	air
Kinematic viscosity	ν [m^2/s]	10^{-6}	$1{,}6 \cdot 10^{-5}$
Total length of fish / airship	L [m]	0.3	1.72
Reynolds number	Re	$0.36 \cdot 10^6$	$1.60 \cdot 10^6$
Fin length	l [m]	0.075	0.3
Flow speed	U [m/s]	1.2	1.5
Strouhal number	Str'	0.45	0.45
Frequency	f [Hz]	4.5	1.4
Peak to Peak amplitude	A_{pp} [m]	0.12	0.48

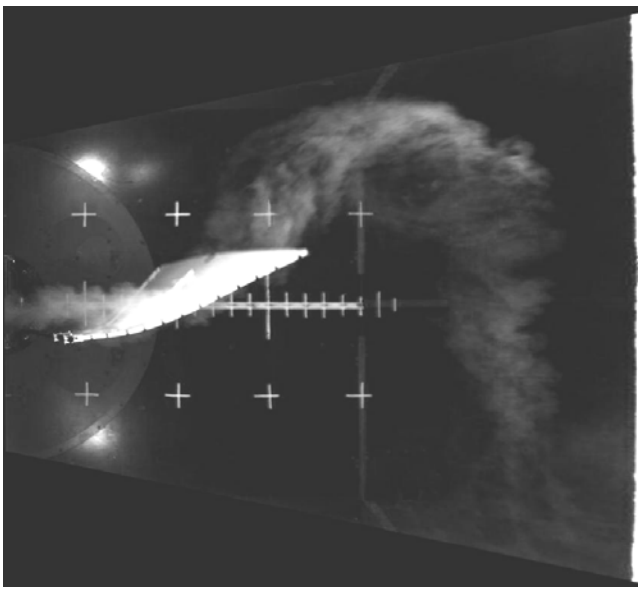

Figure 13. Fin B in the wind tunnel with vortexes generated in the wake (side view).

Our biomimetic airship allowed to exploring scientifically the biomimetic propulsion system in flight tests. This model was equipped with three different flexible fish-like tail-fins instead of the cross-tail. One was a small tuna-shaped tail fine adopted from the fish "Scomber Japonicus ", and two sizes of the trout-like tail fin were tested, see Fig. 16.

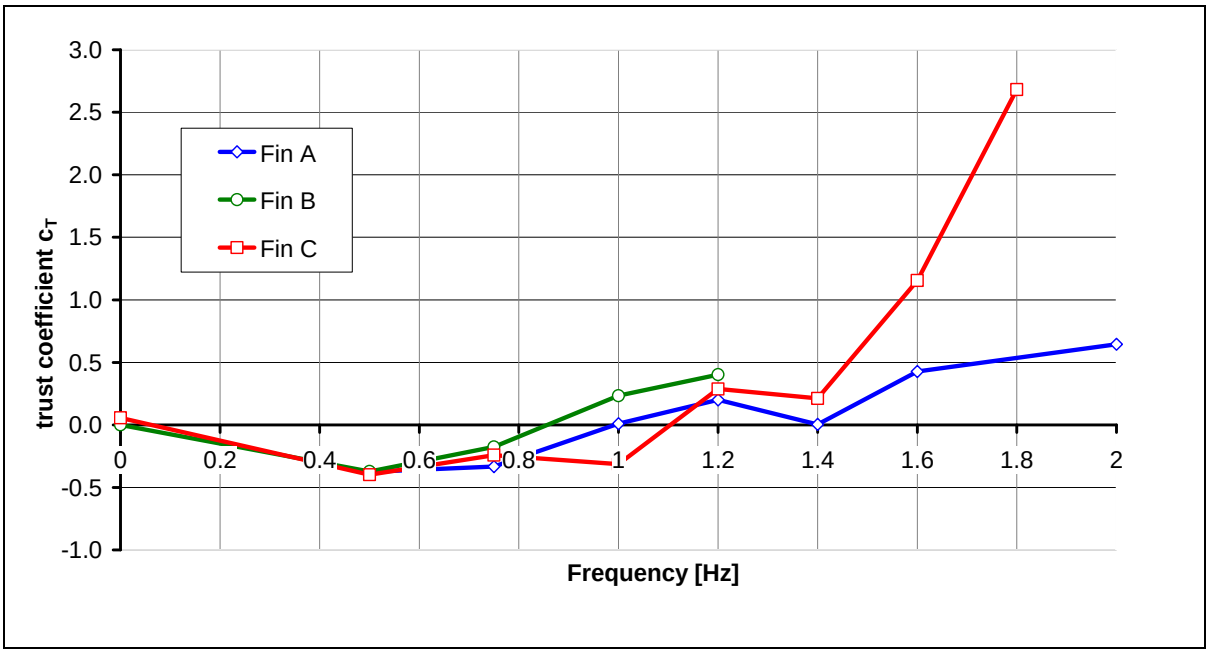

Figure 14. Dimensionless drag/propulsion force versus frequency.

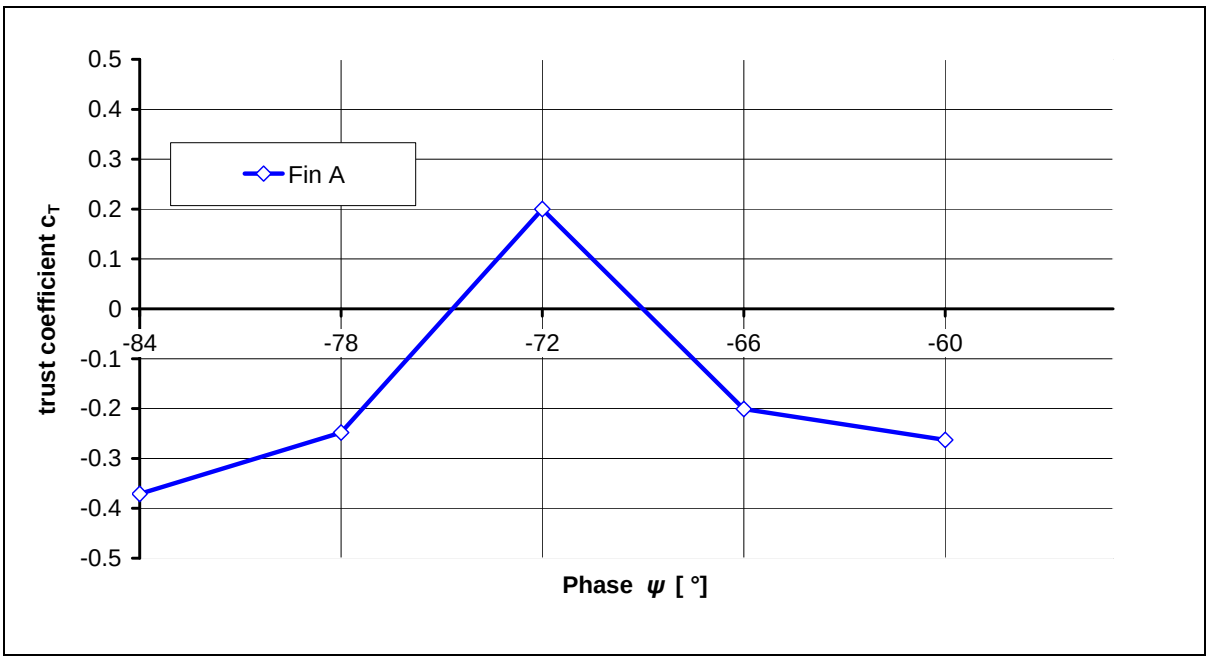

Figure 15. Dimensionless drag/propulsion force versus phase shift for fin A at the design point.

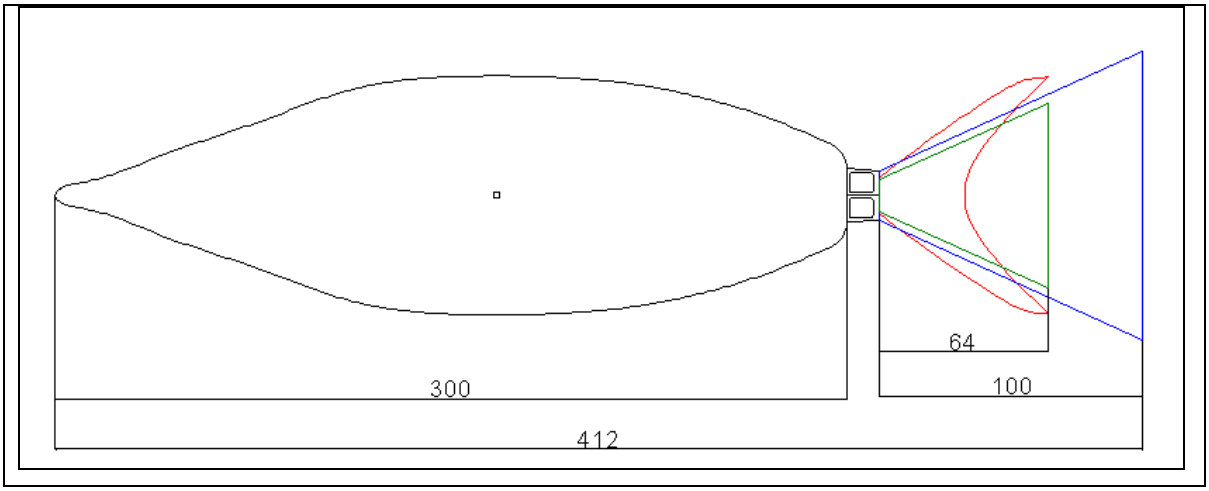

Figure 16. Shape and size of the tail-fins tested in flight tests (red: tuna-shaped, green: small trout-shaped ("B20", "B21", "B24") blue: large trout-shaped "B30").

"B24" was identical in size and shape as the fin B evaluated in the wind tunnel. The large one ("B30") was scaled correctly in respect to the relative size of the tail-fin shown in Fig. 5. These tail-fins were mounted with a hinge at the end of the body, see Fig. 17. With a conventional servo motor this tail-fin was driven such that an undulatoric flapping motion of the root of the fin was realized. Various amplitudes (±12.5°, ±20°, ±30°) and frequencies (0.5 – 2 Hz) could be applied. In total eight different fins, with different shapes, sizes and stiffness were tested in flight. The flight motion was qualitatively judged with respect to stability and the cruising speed was measured.

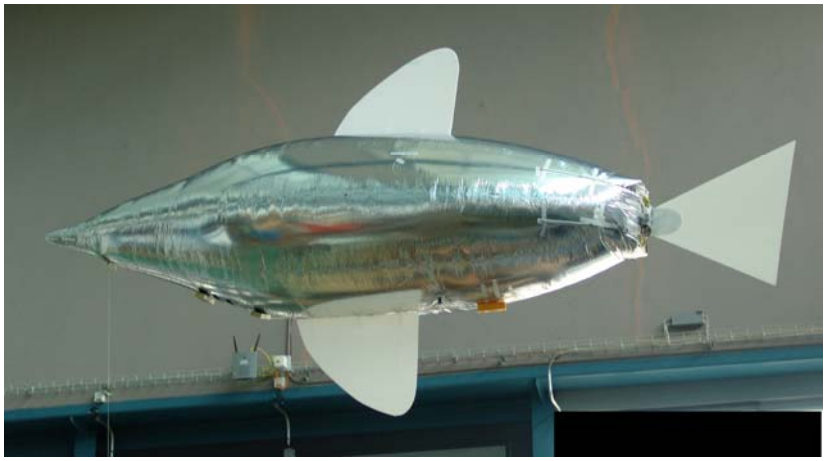

Figure 17. Functional model of a biomimetic airship.

The effect of shape, size and stiffness on the speed of the airship at various frequencies could be quantified. All of these design parameters have a significant effect on the cruising speed. The speed is increasing with increasing frequencies (and increasing amplitude) as well as with increasing stiffness of the tail-fin, sees Fig. 18. A maximum speed of 1.55 m/s could be reached at a Strouhal number of 0.2.

As Wiguna has reported for fish-swimming in [37], we can also conclude for our biomimetic airship, that the total area and the aspect ratio have a significant influence on the speed. McHenry [38] concluded from fish observations, that fish do control their speed by varying their body motion pattern. In the design of the biomimetic airship the resulting motion pattern is crucial for an optimal speed. Therefore the stiffness of the fin plays an important role in the design of a biomimetic airship.

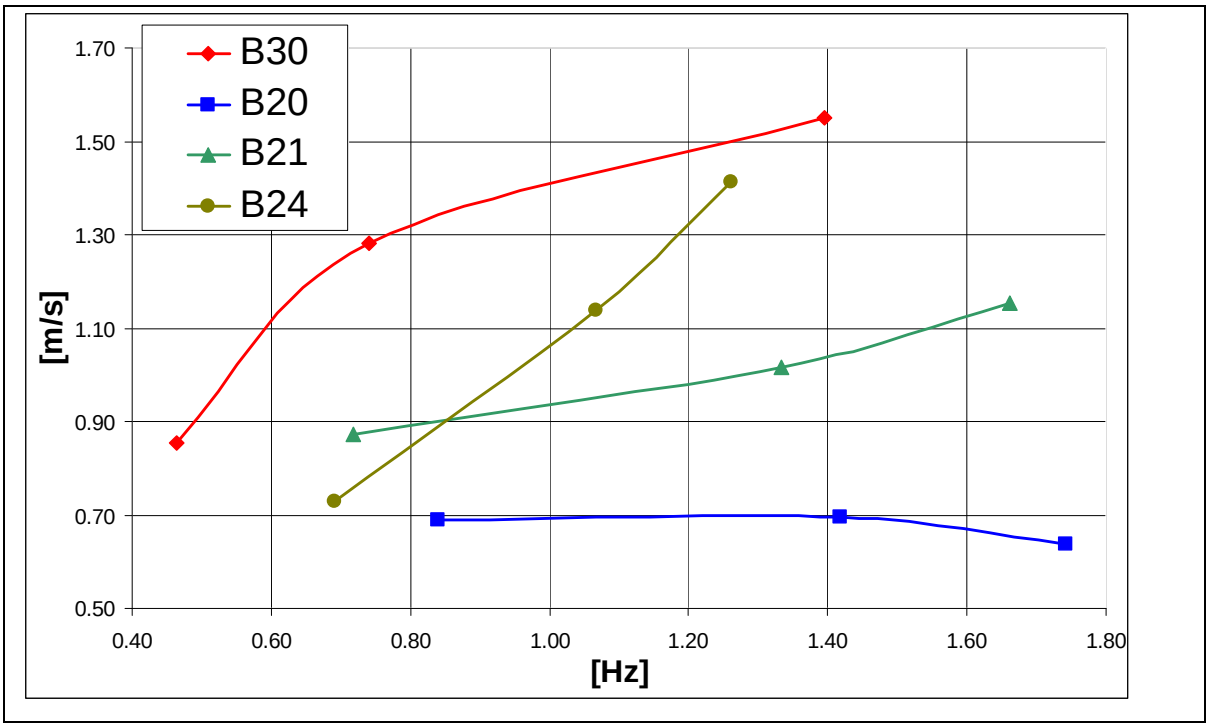

Figure 18. Cruising speed versus flapping frequency for different sizes and stiffnesses of trout-shaped fins: "B30": large, moderate stiff fin, "B20" small, low stiff fin, "B21": small, moderate stiff fin, "B24": small, high stiff fin.

3-5. Open questions and future work

The major task in the near future will be the structural technology of the active body. Detailed design studies on structural configurations and the definition of the distribution of active body segments to generate the required bending deformation have already started. So far the experiments with semi-rigid bending body segments, the required bending angle could not yet be reached under standard operational conditions. The manufacturing process for these active segments is still unsatisfactory. The primarily hand-made active hull segments show still a rather poor reliability and the reproducibility has to be improved significantly by using industrial fabrication processes.

Due to the fact, that we have not yet the methods available to fully simulate the structural mechanics and the fluid-dynamics the empirical approach is very important in this project. We will continue to explore the structural behaviour of active membranes in experiments, as well as the fluid-dynamic performances of the fins and the whole airship in wind tunnel tests or flight trials. Optimization of the whole system of a biomimetic airship will be the subject of long-time research, also in our group.

4. CONCLUSIONS

The proposed concept of a biomimetic airship is a highly multidisciplinary challenge. Many aspects, such as aerodynamics, aerostatics and structural mechanics have to be fulfilled in order to be a functional solution. For many of these design criteria the methods have not yet been developed in detail. However, if there is a combination of active bending body segments, tail fin actuation and aero-elastic tail fin a more energy efficient, noiseless and environmental friendly transport system would be possible.

ACKNOWLEDGEMENTS

The flow simulations performed by Manfred Quack, Dr. Stefan Kern and Prof. Petros Koumoutsakos at the Chair of Computational Science of ETH Zurich are greatly acknowledged.
The support by Dr. Stefano Airaghi in the wind tunnel tests on tail fins at the Institute of Fluiddynamics at ETH Zurich is greatly acknowledged.
We thank Christian Gephardt from AeroiX GmbH for the design, manufacturing of the various envelopes and Martin Wähmer from the Institute of Aeronautics and Astronautics, TU Berlin for the evaluation of the overall performance of the "airfish 3.10" design.

The project has been financed by the board of directors of Empa.

REFERENCES

1. Yu, J., Tan, M., Wang, S. and Chen, E., "Development of a Biomimetic Robotic Fish and its Control Algorithm", *IEEE Transactions on Systems, Man, and Cybernetics - Part B: Cybernetics*, 34(No 4), (2004)
2. Tan, X., Kim, D., Usher, N., Laboy, D., Jackson, J., Kapetanovic, A., Rapai, J., Sabadus, B. and Zhou, X., "An Autonomous Robotic Fish for Mobile Sensing"
3. Wang, H., Tjahyono, S.S., MacDonald, B., Kilmartin, P.A., Travas-Sejdic, J. and Kiefer, R., "Robotic Fish Based on a Polymer Actuator."
4. Wang, T., Liang, J., Shen, G. and Tan, G., "Stabilization based design and experimental research of a fish robot."
5. Michel, S., Lochmatter, P. and Kovacs, G. Konzept einer alternativen Antriebsart für Prallluftschiffe. *DGLR Workshop Leichter-als-Luft*, pp. 1383 - 1388 (DGLR, Friedrichshafen, 2005).
6. Warwick, G., "Return of the Airship." *Flight International*, 15. - 21. August. 2006, (2006).
7. Apel, U., "Stratospheric Platforms a definition study for a ESA platform." *ESA*, (2005).
8. Information on http://www.sanswire.com
9. Information on http://www.gefa-flug.de
10. Lavie, A., "FP6-2002-AERO-2 SSA Project - Contract No 516081 - USE HAAS - Final Technical Report - Executive Summary of the Project." (2006).
11. Hertel , H. "*Struktur - Form - Bewegung*." (Krauskopf-Verlag, Mainz, (1963).
12. Bannasch, R., "Drag Minimisation on Bodies of Revolution in Nature and Engineering." *1. Int. Airship Conference*, pp. 79-87Stuttgart, (1993).
13. Bannasch, R., "Widerstandsarme Strömungskörper - Optimalformen nach Patenten der Natur" *BIONA-report*, 10, pp. 151 - 177, (1995).
14. Michel, S., Kovacs, G. and Lochmatter, P., "Propulsion Unit for Lighter-than-Air Aircraft", CH, (2006).
15. Fish, F.E. and Lauder, G.V., "Passive and Active Flow Control by Swimming Fishes and Mammals", *Annu. Rev. Fluid Mech.*, 38, pp. 193-224, (2006).

16. Sfakiotakis, M., Lane, D.M. and Davies, J.B.C., "Review of fish swimming modes for aquatic locomotion", *IEEE J of Oceanic Engineering*, 24(2), pp. 237-711, (1999).
17. Triantafyllou, M.S. and Triantafyllou, G.S., "An efficient swimming maschine", *Scientific American*, Mar 95(3), (1995)
18. Guillaume, N., Benoit, B., Briac, C. and Berton, E., "How are Strouhal number, drag, and efficiency adjusted in high level underwater monofin-swimming?", *Human Movement Science*, 26, (2007)
19. Rohr, J.J. and Fish, F.E., "Strouhal numbers and optimization of swimming by odontocete cetaceans", *The Journal of Experimental Biology*, 207, (2004)
20. Taylor, G.K., Nudds, R.L. and Thoams, A.L.R., "Flying and swimming animals cruise at a Strouhal number tuned for high power efficiency", *Nature*, 2003, 425, (16. Oct. 2003)
21. Nägele, T., "Bioaquatische Lokomotion: Charakterisierung und Übertragung auf für Leichter-als-Luft-Flugsysteme", *Inst. für Statik und Dynamik der Luft- und Raumfahrtkonstruktionen*, p. 90, Stuttgart, (2006).
22. Kern, S. and Koumoutsakos, P., "Simulations of Optimized Anguilliform Swimming", *Journal of Experimental Biology*, 209, pp. 4841 - 4857, (2006).
23. Nauen, J.C. and Lauder, G.V., "Quantification of the wake of rainbow trout (Oncorhynchus mykiss) using three-dimensional stereoscopic digital particle image velocimetry", *J of Experimental Biology*, 205, 9, (2002).
24. Webb, P.W., "Is the High Cost of body/caudal fin undulatory swimming due to increased friction drag or inertial recoil", *J. of Exp. Biology*, 162, pp. 157-166 (1992).
25. Müller, U.K., Smit, J., Stamhuis, E.J. and Videler, J.J., "How the body contributes to the wake in undulatory fish swimming: Flow fields of a swimming eel (Anguilla Anguilla)", *Journal of Experimental Biology*, 204, 12, (2001).
26. Information on http://muenster-uni.biokon.net/finray/finray.htm
27. Clark, R.P. and Smits, A.J., "Thrust production and wake structure of a batoid-inspired oscillating fin", *Journal of Fluid Mechanics*, 562, 15., (2006)
28. Bar-Cohen, Y., "*Electroactive polymer (EAP) actuators as artificial muscles : reality, potential, and challenges*", (SPIE Press, Bellingham, Washington, (2004).
29. Bernasconi, M., Michel S., Ermanni P., "Feasability study for an Active Envelope based on Electroactive Polymers for a Blimp", Diploma Thesis, ETHZ (ETH, Zürich, 2007).
30. Quack, M., Kern, S., Michel, S. and Koumoutsakos, P., "Simulations of airships at low Reynolds numbers", (in preparation).
31. Hitz, R., Binsteiner, M. and Michel, S., "Machbarkeitsstudie und Vorentwicklung für ein aktives Scharnier auf EAP-Basis", *Inst. für Virtuelle Produktion*, p. 86 (ETH, Zürich, 2006).
32. Lochmatter, P. and Kovacs, G., "Design and characterization of an active hinge segment based on soft dielectric EAPs", *Sensors and Actuators A: Physical*, A141(2), pp. 577-587, (2008).
33. Anderson, J.M., Streitlien, K., Barrett, D.S. and Triantafyllou, M.S., "Oscillating Foils of High Propulsive Efficiency", *J. Fluid Mech.*, 360, pp. 41 - 72, (1998).
34. Bandyopadhyay, P.R., "Trends in Biorobotic Autonomous Undersea Vehicles. *IEEE Journal*

of Ocean Engineering, 30(1), PP 109 - 139, (2005).

35. Information on http://www.festo.com

36. Schwan, S. and Just, D., "Wall-Halla - Gala-Show der Indoorflieger", *modellflieger*, Febr./März 2008, (2. 2008).

37. Wiguna, T., Park, H.C., Heo, S. and Goo, N.S., "Experimental parametric study of a biomimetic fish robot actuated by piezoelectric actuators", in Bar-Cohen, Y., ed. *SPIE EAPAD,* San Diego, (2007).

38. McHenry, M.J., Pell, C.A. and Long, J.H., "Mechanical Control of Swimming Speed -Stiffness and Axial Wave-Form in Undulating Fish Models", *Journal of Experimental Biology*, 198(11), (12. 1995).